The Medial Amygdalar Nucleus: A Novel Glucose-Sensing Region That Modulates the Counterregulatory Response to Hypoglycemia

Ligang Zhou,[1] Nina Podolsky,[2] Zhen Sang,[1] Yuyan Ding,[1] Xiaoning Fan,[1] Qingchun Tong,[3] Barry E. Levin,[2] and Rory J. McCrimmon[1,4]

OBJECTIVE—To determine whether the medial amygdalar nucleus (MAN) represents a novel brain glucose-sensing region involved in the detection of hypoglycemia and generation of a counterregulatory hormone response.

RESEARCH DESIGN AND METHODS—Fura-2 calcium imaging was used to assess glucose responsivity in neurons isolated from the MAN and single-cell real-time reverse transcription PCR used to examine gene expression within glucose-responsive neurons. In vivo studies with local MAN perfusion of the glucoprivic agent, 2-deoxyglucose (2-DG), under normal and hypoglycemic conditions and also after MAN lesioning with ibotenic acid, were used to examine the functional role of MAN glucose sensors. In addition, retrograde neuronal tracer studies were used to examine reciprocal pathways between the MAN and the ventromedial hypothalamus (VMH).

RESULTS—The MAN contains a population of glucose-sensing neurons (13.5%), which express glucokinase, and the selective urocortin 3 (UCN3) receptor CRH-R2, but not UCN3 itself. Lesioning the MAN suppressed, whereas 2-DG infusion amplified, the counterregulatory response to hyperinsulinemic hypoglycemia in vivo. However, 2-DG infusion to the MAN or VMH under normoglycemic conditions had no systemic effect. The VMH is innervated by UCN3 neurons that arise mainly from the MAN, and ~1/3 of MAN UCN3 neurons are active during mild hypoglycemia.

CONCLUSIONS—The MAN represents a novel limbic glucose-sensing region that contains characteristic glucokinase-expressing glucose-sensing neurons that respond directly to manipulations of glucose availability both in vitro and in vivo. Moreover, UCN3 neurons may provide feedback inhibitory regulation of the counterregulatory response through actions within the VMH and the MAN. ***Diabetes*** **59:2646–2652, 2010**

From the [1]Department of Internal Medicine, Yale University, New Haven, Connecticut; the [2]VA Medical Center, Neurology Service, East Orange, New Jersey; the [3]Department of Internal Medicine, Beth Israel Deaconness Medical Center, Boston, Massachusetts; and the [4]Biomedical Research Institute, University of Dundee, Dundee, Scotland.

Corresponding author: Rory J. McCrimmon, r.mccrimmon@dundee.ac.uk.

Received 7 July 2009 and accepted 5 July 2010. Published ahead of print at http://diabetes.diabetesjournals.org on 13 July 2010. DOI: 10.2337/db09-0995.

In some patients with type 1 (and 2) diabetes, the ability to detect and respond to hypoglycemia is markedly impaired (1). Specialized glucose-sensing neurons exist within discrete regions of the brain and are thought to have a particular role in the regulation of glucose homeostasis. Glucose-excited neurons increase their activity as glucose levels rise, and glucose-inhibited neurons increase their activity as glucose levels fall (2,3). The mechanisms used by glucose-excited neurons to detect a fall in the glucose level to which they are exposed are thought to resemble those used by the classical glucose sensor, the pancreatic β-cell, with in particular roles for glucokinase and the ATP-sensitive potassium channel (K_{ATP}) (1), while glucose-inhibited neurons also use glucokinase, as well as nitric oxide and adenosine 5′-monophosphate-activated protein kinase to modulate their glucose sensing (4–6). Glucose-sensing neurons are located in a number of brain regions, although only those present in the ventromedial (VMH) (7–9), dorsomedial, and paraventricular hypothalamus (10,11) to date have been shown in vivo, in rodent models, to modulate counterregulatory responses during insulin-induced hypoglycemia.

We have recently shown that urocortin 3 (UCN3), a member of the corticotrophin-releasing hormone (CRH) family of neuropeptides, and a selective ligand for the CRH-R2 receptor, may regulate the magnitude of the counterregulatory response to hypoglycemia through actions in the VMH (12,13). UCN3 nerve terminals provide a dense innervation to the shell of the VMH and tubercle area (14). The cell bodies of UCN3 neurons are found predominantly in the medial amygdalar nucleus (MAN), the hypothalamic medial preoptic nucleus, and the rostral perifornical area lateral to the paraventricular hypothalamic nucleus (14). Intriguingly, the pancreatic isoform of glucokinase, the rate-limiting step of glucose oxidation and a key step in the glucose-sensing mechanism (2,6), is also expressed in the MAN (15). This study examined the hypothesis that the MAN may represent a novel central glucose-sensing region and, moreover, that it might be directly linked with the VMH via UCN3 neurons.

RESEARCH DESIGN AND METHODS

Male Sprague-Dawley rats (mean ± SEM wt, 305 ± 4 g) were housed in the local Animal Resource Center with water and chow pellet available ad libitum. The animal care and experimental protocols were reviewed and approved by Yale University Institutional Animal Care and Use Committee and the Institutional Animal Care and Use Committee of the East Orange Veterans Affairs Medical Center.

Animal surgery. The surgical procedures used in this study have been described in detail elsewhere (8,16). In brief, one week prior to each study, all animals were anesthetized with an intraperitoneal injection (1 ml/kg) of a mixture of xyzaline (20 mg/ml; AnaSed, Lloyd Laboratories Inc.) and ketamine (100 mg/ml; Ketaset, Wyeth) at a ratio of 1:2 (vol/vol). Vascular catheters [PE50 tubing with a tip made from silastic laboratory tubing (0.51 mm inner diameter)] were inserted via a neck incision into the internal jugular vein and carotid artery. After catheter implantation, cannula guides were stereotaxically inserted, bilaterally to the MAN (coordinates from bregma, anterior-posterior [AP] = −2.80 mm, medio-lateral [ML] = ±3.3 mm, and dorso-ventral [DV] = 8.9 mm at an angle of 90°) or VMH (coordinates AP = −2.6 mm; ML = ±0.5 mm; DV = 9.4 mm). Guide cannula were designed to reach a point 1 mm proximal to the target nucleus, limiting gliosis in the region where microinjection would take place 7 days after guide catheter insertion.

Lesion study. At the initial surgery, as described above, and instead of guide cannula insertion, each rat received bilateral microinjections to the MAN of 2 pg of ibotenic acid ($n = 6$) using a 1 μl Hamilton syringe (total volume 200 nl over 30 min), after which the skin was closed with wound clips. Sham-lesion rats received the identical surgical procedure but were administered saline rather than ibotenic acid ($n = 9$).

Normoglycemic study. Seven days after surgery, overnight fasted rats had their catheters opened and were allowed to acclimatize over 90 min. Bilateral 26-guage injection needles, designed to extend 1 mm beyond the tip of the guide cannula, were then inserted into each MAN or VMH, and each rat received bilateral microinfusions (1 μl given at a rate of 0.033 μl/min for 30 min) of 10 mmol/l 2-deoxyglucose (2-DG), a nonmetabolizable form of glucose that creates local glucopenia, or artificial extracellular fluid (aECF), depending on the study. Venous samples for measurement of plasma glucose were taken every 10 min and for glucagon and epinephrine preinjection ($t = 0$ min) and at 30 and 60 min after microinjection.

Hyperinsulinemic hypoglycemic study. A modified hyperinsulinemic glucose clamp was used to produce a standardized hypoglycemic stimulus, as described previously (17). Thirty min after bilateral MAN microinfusions of 2-DG ($n = 6$) or artificial aECF ($n = 9$), a constant 20 mU/kg/min infusion of insulin (Human Regular Insulin, Lilly, IL) was started. Both solutions were mixed with 4% wheat germ agglutinin (WGA) to confirm the location of microinjection (supplementary Fig. 1, available in an online appendix at http://diabetes.diabetesjournals.org/cgi/content/full/db09-0995/DC1). The plasma glucose was allowed to fall to 70 mg/dl (~3.9 mmol/l), where it was maintained for 90 min using 20% dextrose, with the dextrose infusion rate adjusted every 5 min based on plasma glucose determinations. Blood samples for measurement of epinephrine, glucagon, and insulin were taken at 0, 60, and 90 min. Plasma glucose was measured by glucose oxidase method (Glucose Direct; Analox Instruments, Lunenberg, MA). Catecholamine analysis was performed by high-performance liquid chromatography using electrochemical detections (ESA, Acton, MA); plasma insulin and glucagon were measured by radioimmunoassay (Millipore, Temecula, CA).

Retrograde neuronal tracer studies. The retrograde tracing technique has been described previously (18). Briefly, each rat was microinjected bilaterally to the VMH or MAN (coordinates as above) with the retrograde neuronal tracer WGA or 4% fluorogold dissolved in aECF and delivered through a glass micropipette with tip diameter 10–15 μm by passing 2-μA positive current pulse (7 s on/off) for <10 min. The rats were then allowed to recover for 7 days before undergoing a 90-min hyperinsulinemic (20 mU/kg/min) hypoglycemic (70 mg/dl) or hyperinsulinemic euglycemic (120 mg/dl) clamp, as described above.

Immunohistochemistry. The immunohistochemistry protocol used has been described in detail previously (18,19). Briefly, analysis was performed on every six 40-μm-thick frontal sections. Sections were washed in PBS for 10 min and then pretreated in 0.3% H_2O_2 for 1 h to block endogenous peroxidase. They were then incubated overnight at room temperature with 1:1,000 rabbit anti-UCN antibody (1:2000; a gift from Dr. W. Vale) in 0.3% fresh normal donkey serum, goat anti-WGA (1:1,000; Vector) and PBT-azide (0.02% sodium azide and 0.04% Triton X-100 in PBS). The next day, sections were incubated with biotinylated donkey anti-rabbit antibody (Jackson Laboratories; 1:500) for 1 h, followed by incubation with a cocktail of Alexa Fluor 594-conjugated Streptavidin (Molecular Probes, Eugene, OR; 1:1K) and Alexa Fluor 488-conjugated chicken anti-goat antibody (1:400) for 1 h. After mounting on polylysine slides, the sections were cover-slipped with antifade mount medium for fluorescence (Vectashield, Vector, CA). Dual fluorescence images in the MAN from the representative brain were taken with a digital camera. Counting of dual staining for UCN3 and WGA was performed in three brains. All single-labeled UCN3 neurons and dual-labeled neurons for UCN3 and WGA in the MAN were counted. Cytoarchitectonic areas in the amygdala were determined with reference to the atlas of Paxinos and Watson (20). Light-microscope images in the MAN and its adjacent regions from a representative brain were taken with a digital camera. The digital images were arranged in the software Canvas (Deneba System, Miami, FL). The border of the MAN, its adjacent structures, and distribution of single labeling of UCN3 neurons were drawn using Canvas software. For triple staining, immunofluorescence serial sections from the brains of fluorogold-injected rats were incubated overnight with a mixture of 1 μg/ml anti-Fos goat antibody (1:1K; Santa Cruz) and anti-UCN3 rabbit serum (1:2,000). After a rinse with PBS-X, the sections were incubated for 1 h with 10 g/ml biotinylated anti-rabbit IgG donkey antibody (Jackson) and then for 1 h with a mixture of 1 μg/ml Alexa488-conjugated chicken anti-goat antibody (1:400; Molecular Probes) and 1 μg/ml Alexa594 Streptavidin-conjugated antibody (Molecular Probes). Sections were observed under an epifluorescence microscope Olympus BX-50 with appropriate filter sets for Alexa488 (excitation, 450–490 nm; emission, 514–565 nm); Alexa594 (excitation, 530–585 nm; emission, ≥615 nm) and fluorogold (excitation, 359–371 nm; emission, 397–590 nm). Although Alexa488 fluorescence could be partially seen with the filter set for fluorogold, Fos-immunoreactive neuropil with Alexa488 fluorescence was easily differentiated from retrograde labeled cell bodies with fluorogold fluorescence. The counting of triple staining for UCN3, Fos, and fluorogold was performed in three brains. All single-labeled UCN3 neurons and dual-labeled and triple-labeled neurons in the MAN were counted.

MAN mRNA assays by quantitative real-time PCR. Frozen brains were cut on a cryostat at −12°C and placed in RNAlater (Ambion, Foster City, CA) until being micropunched. Micropunches of the MAN were performed by modifications of the method of Palkovits (21), where brain micropunches are made under microscope guidance from brain slices placed on the base of a stereotaxic frame. Micropunched brain areas were sonicated in a guanidinium thiocyanate solution and purified using magnetic beads (Ambion MagMax-96). Quantitation of mRNA was carried out by real-time quantitative PCR (QPCR) as previously described (22). Primer sets for each mRNA were designed by reference to published sequences, and their specificity was verified using Genebank. Primers and their sequence-specific FAM-labeled probes prepared by Applied Biosystems were sequenced and then quantified with an Applied Biosystems 7,700 real-time PCR system set for 40 PCR cycles. Standard curves were generated from serially diluted pooled samples for each probe and for constitutively expressed mRNA (cyclophilin) to control for differences in amplification efficiency and micropunch size. Results were calculated from the standard curves relative to cyclophilin mRNA levels in the same samples.

Fura-2 calcium imaging to assess glucose-induced changes in intracellular calcium ($[Ca^{2+}]_i$) oscillations. Studies were carried out in 3–4 week old male Sprague-Dawley rats (Charles River). The MAN punched cells were dissociated with papain (2 mg/ml, 30 min, 37°C) and mechanically triturated. Cells were plated onto cover slips and allowed to adhere for 60 min before loading with the Ca^{2+} fluorophore fura-2 acetoxy methyl ester (Molecular Probes) for 20 min in Hank's balanced salt solution buffer containing 2.5 mmol/l glucose, washed twice, and transferred to a microscope chamber held at 37°C. Fura-2 fluorescent images were acquired every 5 s by alternating excitation at 340 and 380 nm using a cooled, charge-coupled device camera at 420–600 nm emission. Changes in glucose were maintained for ~10 min after addition. Cells were classified as glucose-responsive in >500 neurons by significant ($[Ca^{2+}]_i$) fluctuations (as area under the curve) after changes in glucose concentrations using Origin 7.0 software (OriginLab). Neurons were classified as glucose-excited, glucose-inhibited, and nonglucosensing, as previously described (7). Cytoplasms of individual characterized neurons were then collected for single-cell QPCR (sc-QPCR) as previously described (23); analysis was according to previous standards.

sc-QPCR. After characterization by Ca^{2+} imaging, cytoplasmic mRNA of individually imaged cells was analyzed by sc-QPCR. Cytoplasm from each neuron was aspirated into a micropipette that was prefilled with DEPC-treated water containing 1 μl RN_{ASE} OUT RNase inhibitor (Invitrogen, Carlsbad, CA). Subsequently, synthesis was performed with Superscript II first-strand synthesis kit (Invitrogen) following the manufacturer's directions. The RT reaction was incubated at 42°C for 50 min after heat inactivation at 70°C. cDNA was purified to completely remove inhibitory RT components by slight modification of the methods described by Liss (24). After the purification of single-cell cDNA, QPCR was performed using specific primers. Glial fibrillary acidic protein was used to exclude astrocytes, and β-actin was used as an internal control for constitutively expressed mRNA. Primer sequences were designed using Biology WorkBench Primer design software. Amplification was carried out in a LightCycler (Roche Perkin-Elmer, Foster City, CA), using 40 cycles (95°C, 1 s; 56–63°C, 2 s; and 68°C, 30 s) with Advantage 2 Polymerase Mix (BD Biosciences, Palo Alto, CA). Amplified products were run directly on a 1.5% agarose gel and visualized by ethidium bromide staining. Gels were imaged and photo inverted for presentation. To optimize conditions for primer amplification and standardize for the linearity of the amplification process, hypothalamic cDNA was used.

For glucagon and epinephrine, differences between treatments were assessed via repeated-measures ANOVA and based on hormonal readings

TABLE 1
Glucose-responsive MAN neurons

Neuron	Number	Percentage
GE	32/522	6%
GI	39/522	7.5%
NG	449/522	86.5%

Fura-2 calcium imaging was used to measure changes in $[Ca^{2+}]_I$ oscillations while varying glucose concentrations 2.5 to 0.5 to 2.5 mmol/l glucose in neurons isolated from the MAN. GE, glucose-excited neuron; GI, glucose-inhibited neuron; NG, glucose-unresponsive neuron.

at 0, 60, and 90 min. Post hoc analysis was made using Bonferroni testing. Mean data were compared using a two-tailed Student *t* test. For all analyses, significance was assigned at the $P \leq 0.05$ level. Data are presented as mean ± SEM.

RESULTS

The MAN contains glucose-sensing neurons. Of 522 individual MAN neurons examined using fura-2 calcium imaging, 13.5% were glucose-sensing (Table 1). Six percent were glucose-excited, and 7.5% were glucose-inhibited (Fig. 1). By sc-QPCR, 54% of glucose-excited, 42% of glucose-inhibited, and 9% of nonglucosensing MAN neurons expressed glucokinase (Table 2). However, UCN3 was isolated from only 2, 16, and 4% of the glucose-excited, glucose-inhibited, and nonglucosensing neurons, respectively.

Glucokinase, CRH-R2, and UCN3 show different spatial relationships within the MAN. Having shown that only a minority of glucose-sensing neurons contained mRNA for UCN3, quantitative real-time PCR was used to examine the spatial distribution of glucokinase, UCN3, and CRH-R2 mRNA expression in MAN micropunches. A rostrocaudal gradient in glucokinase, UCN3, and CRH-R2 gene expression in the MAN was seen. Both glucokinase and CRH-R2 expression showed a similar rostrocaudal distribution, whereas UCN3 showed the opposite rostrocaudal distribution in the MAN (supplementary Fig. 2, available in an online appendix).

Lesioning the MAN results in a suppressed counterregulatory hormonal response to acute hypoglycemia. To examine whether the MAN contributed to the generation of a counterregulatory response during acute hypoglycemia in vivo, the MAN of male Sprague–Dawley rats was lesioned by direct microinjection of ibotenic acid.

TABLE 2
Glucokinase and UCN3 mRNA expression in glucose-excited, glucose-inhibited, and glucose-unresponsive neurons in the MAN identified by Fura-2 calcium imaging, revealed by single-cell RT-PCR

Neuron	Number	Co-expressing with GK	Co-expressing with UCN3
GE	46	54%	2%
GI	45	42%	16%
NG	23	9%	4%

GE, glucose-excited neuron; GI, glucose-inhibited neuron; GK, glucokinase; NG, glucose-unresponsive neuron.

During the subsequent hyperinsulinemic hypoglycemia study, plasma glucose levels did not differ between MAN lesioned and control rats (70 ± 1 vs. 69 ± 1 mg/dl, respectively; Fig. 2*A*). Glucose infusion rates (GIR) required to maintain the hypoglycemic plateau were ~18% higher in MAN-lesioned rats (mean GIR over 60–90 min, 24.7 ± 1.7 vs. 20.3 ± 1.4 mg/kg/min), although the overall interaction was not significant ($F = 4.0$; $P = 0.07$; Fig. 2*B*). However, MAN lesioning did result in significantly impaired plasma epinephrine ($F = 6.0$, $P < 0.05$) and glucagon ($F = 6.9$, $P < 0.05$) responses to the hypoglycemic challenge (Fig. 2*C* and *D*).

Localized glucoprivation in the MAN and VMH in the fasting state has no effect on glucose counterregulation. To determine whether the MAN might respond directly to a local glucoprivic challenge, the MAN was locally perfused with 2-DG over 30 min. MAN glucoprivation did not result in a significant rise in plasma glucose or change in plasma levels of glucagon and epinephrine (Table 3). Application of 2-DG at an identical concentration and rate to the VMH also failed to elicit a glucoprivic response (Table 3). Additional studies injecting 5-Thioglucose (a more potent glucoprivic agent) into the MAN or VMH also had no significant effect on glucose or counterregulatory hormones (data not shown).

MAN glucoprivation during mild systemic hypoglycemia amplifies the counterregulatory response. In contrast to the lack of effect of local MAN glucoprivation during euglycemia, comparable MAN glucoprivation during mild systemic hypoglycemia did alter the subsequent counterregulatory response. Despite equivalent hypoglycemia [mean (SEM) 60–90 min glucose levels, 70 ± 2

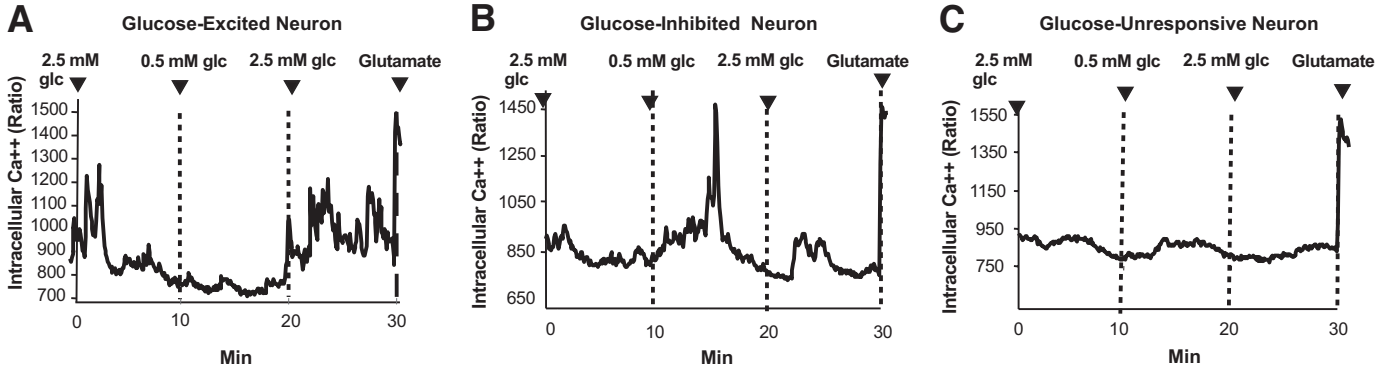

FIG. 1. Representative changes in $[Ca^{2+}]_i$ oscillations after exposure to incremental dose glucose in freshly dissociated medial amygdalar neurons from 3–4-week-old male Sprague–Dawley rats. All recordings were carried out in 2.5 mmol/l glucose (2.5 mmol/l glc) followed by two doses of glucose (0.5 and 2.5 mmol/l), and then tested with glutamate. *A*: Glucose-excited neuron ($n = 25$) showing increased $[Ca^{2+}]_i$ oscillations at 2.5 mmol/l, decreased $[Ca^{2+}]_i$ oscillations at 5 mmol/l, and a robust response to glutamate. *B*: Glucose-inhibited neuron ($n = 27$) showing low $[Ca^{2+}]_i$ oscillations at 0.5 mmol/l and substantial response at 2.5 mmol/l. *C*: Neuron unresponsive to different physiological levels of glucose ($n = 14$).

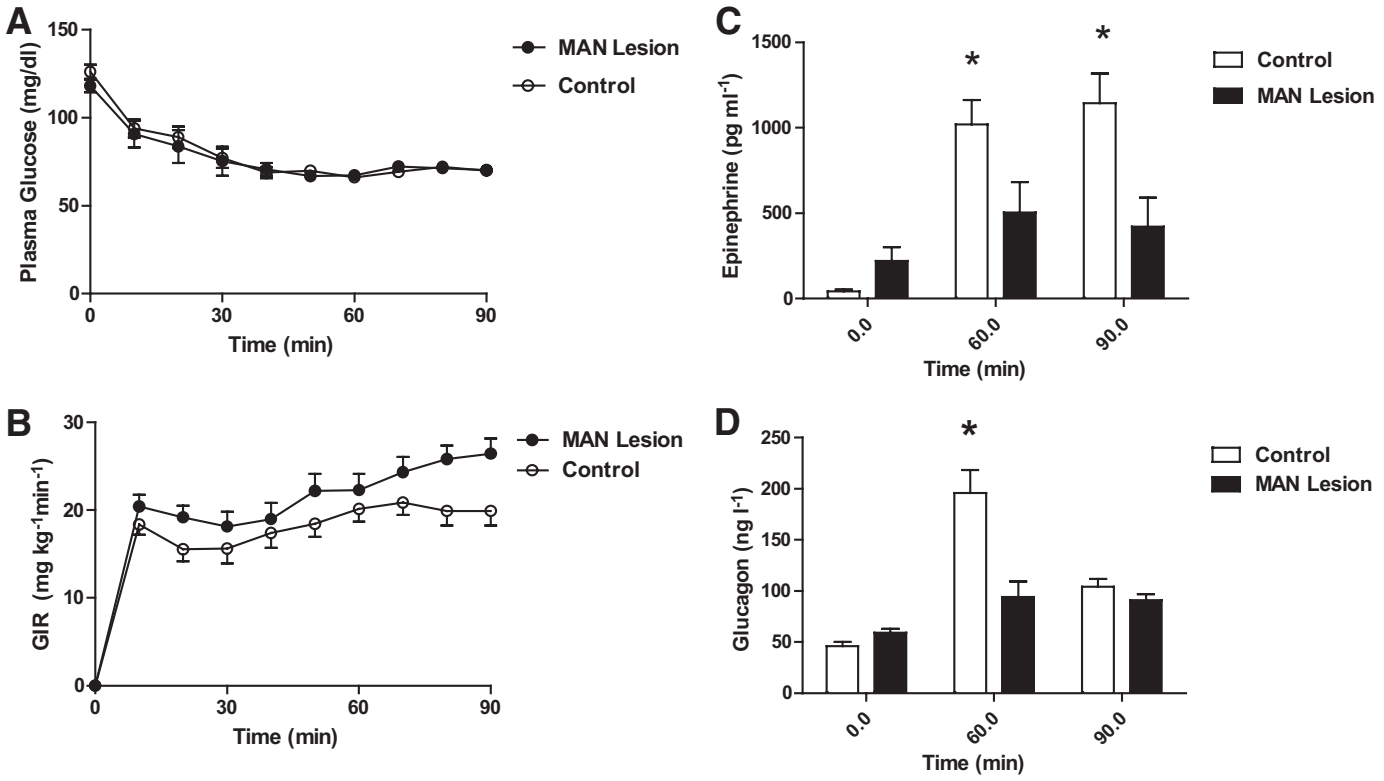

FIG. 2. Lesioning of the MAN leads to suppression of counterregulatory responses to acute hypoglycemia. *A*: Declines in plasma glucose level in response to the hyperinsulinemic clamp (70 mg/dl) did not differ between control (white circle) and MAN lesion (black circle) groups. *B*: Decreased need for exogenous glucose (decreased glucose infusion rate [GIR]) after MAN lesion. *C*: Suppressed epinephrine and (*D*) glucagon secretory responses to hypoglycemia after MAN lesion. Data are expressed as mean ± SE.

versus 69 ± 1 mg/dl (3.9 ± 0.1 vs. 3.9 ± 0.1 mmol/l); Fig. 3*A*], GIR (60–90 min) were threefold lower in the MAN 2-DG infused rats compared with the aECF control group (3.8 ± 1.1 versus12.3 ± 2.2 mg/kg/min, respectively; $F = 24.6$, $P < 0.01$) (Fig. 3*B*). Consistent with the lower GIR, 2-DG microinjection to the MAN significantly amplified the glucagon ($F = 4.8$, $P < 0.05$) and epinephrine ($F = 7.2$, $P < 0.05$) responses during hypoglycemia (Figs. 3*C* and *D*).

UCN3 neurons innervating the VMH arise primarily from the MAN. To determine the origin of UCN3 neurons innervating the VMH, the retrograde neuronal tracer, WGA, was microinjected into the VMH. While UCN3 neurons are present in the medial preoptic nucleus and the rostral perifornical area as expected, by double-label immunohistochemistry, that most of the UCN3 neurons in the MAN project to the VMH (cell bodies positive for [WGA+UCN3]/UCN3 = 492/520). Moreover, microinjection of a retrograde tracer to the MAN demonstrated direct neural pathways in the reciprocal direction from cell bodies in the VMH to nerve terminals in the MAN (supplementary Fig. 4). A schematic representation of the location of UCN3 cell bodies innervating the VMH is shown in Fig. 4, whereas microphotographs of cells showing dual labeling of UCN3 and WGA in the MAN are shown in supplementary Fig. 3.

Hypoglycemia activates VMH-projecting MAN UCN-3 neurons. To determine whether the UCN3 cell bodies in the MAN were activated during acute hypoglycemia, rats underwent hyperinsulinemic hypoglycemic (~70 mg/dl) or hyperinsulinemic euglycemic (~120 mg/dl) clamp studies for 120 min as described above. Using triple fluorescence immunostaining for cFOS, UCN3, and the retrograde tracer fluorogold, we found that ~30% (155/520 neurons) of those UCN3 neurons in the MAN that innervate the VMH coexpressed cFOS, a marker of neuronal activation, during acute hyperinsulinemic hypoglycemia when compared with hyperinsulinemic euglycemia (1/655; $P < 0.05$). This suggests that at least one-third of the MAN UCN3 neurons are activated during a mild hypoglycemic stimulus (Fig. 5).

TABLE 3
Microinfusion of the nonmetabolizable glucose analog 2-DG to the VMH and MAN of rats following an overnight fast had no effect on plasma glucose or counterregulatory hormones

	MAN + 2-DG ($n = 6$)		VMH + 2-DG ($n = 4$)	
	0 min	60 min	0 min	60 min
Glucose (mg/dl)	114 ± 6	114 ± 7	124 ± 3	112 ± 4
Glucagon (ng/l)	51 ± 3	81 ± 16	72 ± 9	58 ± 9
Epinephrine (pg/ml)	235 ± 66	249 ± 99	208 ± 56	70 ± 45

DISCUSSION

The principal finding of the current study is the novel discovery that the MAN contains glucose-sensing neurons that can influence the magnitude of the counterregulatory response to insulin-induced hypoglycemia. The amygdala is a complex structure, containing a number of discrete nuclei involved in a wide range of behavioral and physiological functions. In the rodent, the MAN is strongly connected with the olfactory system, has numerous interconnections with other amygdalar nuclei (enabling it to integrate the neural outputs from these different regions), and, like the VMH, has also been shown to integrate with

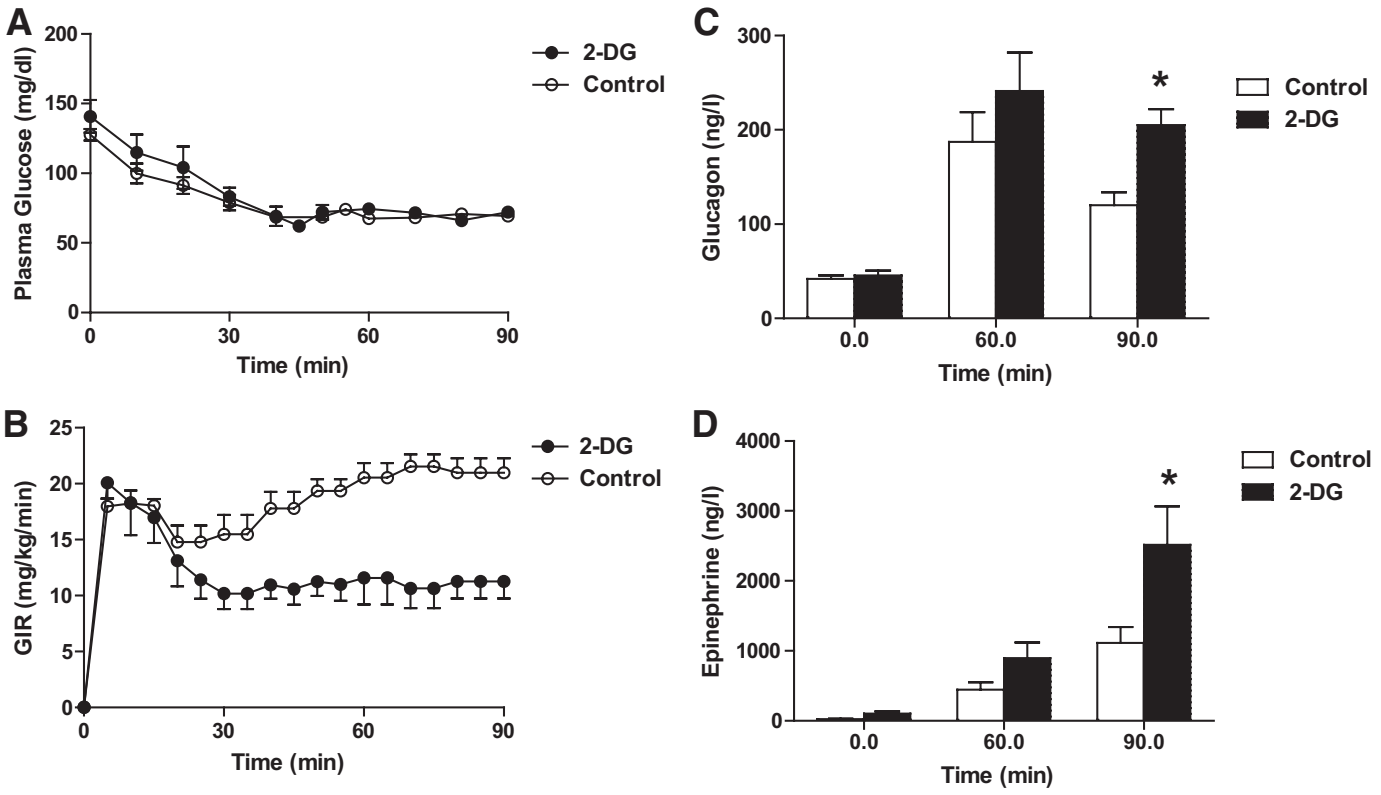

FIG. 3. Provision of an additional glucoprivic stimulus to the MAN amplifies the counterregulatory response to a mild systemic insulin-induced hypoglycemic challenge. *A*: Declines in plasma glucose level in response to the hyperinsulinemic clamp (70 mg/dl) did not differ between control (white circle) and 2-DG (black circle) groups. *B*: Decreased need for exogenous glucose (decreased glucose infusion rate [GIR]) after 2-DG injection into the MAN. *C*: Amplified epinephrine and (*D*) glucagon secretory responses to hypoglycemia in MAN 2-DG injected rats. Data are expressed as mean ± SE.

the neural circuits linked to feeding and body weight control (25,26). Interestingly, a recent study using [^{18}F]-fluorodeoxyglucose positron emission tomography, in 13 men with type 1 diabetes, reported reduced [^{18}F]-fluorodeoxyglucose uptake in the amygdala during hypoglycemia in those subjects with hypoglycemia unawareness failure, suggesting a potential role for the amygdala in the development of hypoglycemia unawareness (27).

The VMH is integral to glucose-sensing during acute hypoglycemia (for a review, see ref [28]). The VMH contains specialized glucose-sensing neurons (23), and 14–19% of these are glucose-excited, whereas 3–14% are glucose-inhibited in type (29). As in the pancreatic β-cell, glucokinase appears to be a critical regulator of glucose-sensing in VMH neurons (6), where glucokinase is expressed in ~65% of glucose-excited and ~45% of glucose-inhibited neurons (23). In fact, it is most likely that all neurons that express glucokinase are actually glucose-sensing and that the finding of glucokinase mRNA in non-glucose-sensing neurons is due to the stringent criteria used to classify neurons. In the present study, we have been able to show, using fura-2-calcium imaging, that the expression of glucokinase mRNA in the MAN is associated with the presence of specialized glucose-sensing neurons. Of these, ~6% were glucose-excited whereas 7.5% were glucose-inhibited. Moreover, 54% of glucose-excited and 42% of glucose-inhibited, compared with only 9% of non-glucose-sensing neurons, contained mRNA for glucokinase. These findings clearly parallel those of the VMH, providing support for the hypothesis that the MAN may represent a novel glucose-sensing brain region.

To determine whether the MAN plays a functional role in glucose-sensing, we initially used the selective neurotoxin, ibotenic acid, to lesion the MAN and then performed a hyperinsulinemic hypoglycemic study. Consistent with a previous study where ibotenic acid was used to lesion the VMH (8), lesioning the MAN was shown to suppress the counterregulatory hormonal response to subsequent hypoglycemia. Subsequently, we sought to determine whether localized glucoprivation in the MAN of euglycemic animals would induce a glucoprivic response, characterized by a rise in plasma glucose and in the counterregulatory hormones glucagon and epinephrine, as previously demonstrated in the VMH (9). However, neither 2-DG nor 5-thioglucose infusions into either the MAN or VMH over 30 min raised plasma glucose, glucagon, or epinephrine levels. We then sought to determine whether combining local MAN glucoprivation during a moderate systemic hypoglycemic stimulus might influence counterregulatory responses to assess whether this additional glucoprivic stimulus might amplify the counterregulatory response. In fact, the combination of local MAN and systemic glucoprivation did have this effect. Taken together, these in vivo studies suggest that the MAN contributes to the counterregulatory response induced by systemic hypoglycemia but that local glucoprivation in the MAN alone is insufficient to generate a counterregulatory hormone response.

A previous study that used unilateral microinjection to localize glucose-sensing brain regions also failed to elicit a glucoprivic response in the majority of hypothalamic regions tested, although it did produce glucoprivic responses with unilateral hindbrain microinjections (30). More recently, bilateral VMH 5-TG microinjections were shown to stimulate food intake; however, no glucose

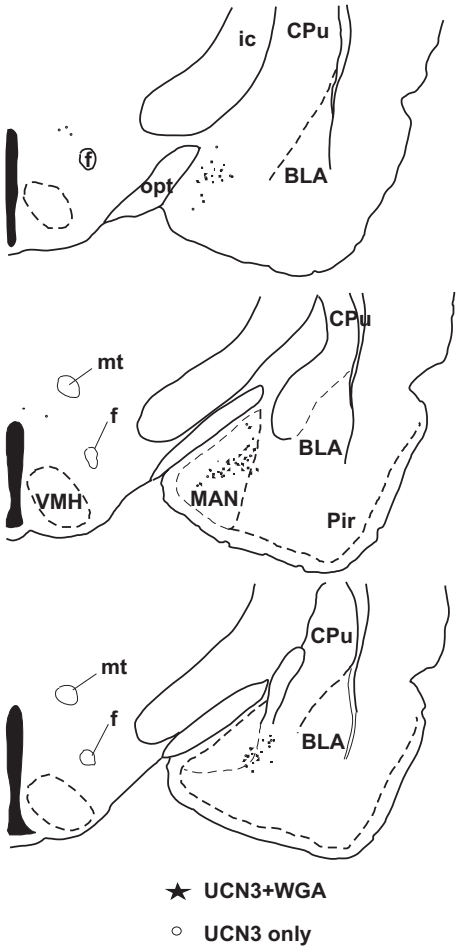

FIG. 4. A schematic diagram illustrating the distribution of UCN3 neurons from serial sections through the MAN. Each open circle represents a neuronal cell body staining for UCN3 alone, while the stars show dual staining for UCN3 and WGA. BLA, basolateral amygdalar nucleus; CPu, caudate putamen (Striatum); f, fornix; ic, internal capsule; mt, mammillothalamic tract; opt, optic tract; Pir, Piriform cortex; PH, posterior hypothalamic nucleus.

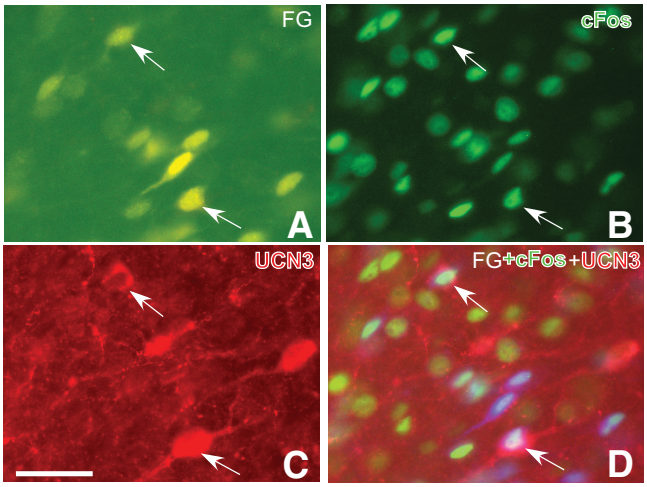

FIG. 5. High magnification image of neuronal cell bodies within MAN. Triple-staining immunohistochemistry was used to indentify UCN3 neurons in the MAN that were activated by hypoglycemia and that directly innervated the VMH. *A*: The retrograde tracer fluorogold (FG) microinjected to the VM and identified as yellow staining within MAN neuronal cell bodies (white arrows). *B*: cFOS immunoreactivity present within MAN neuronal cell bodies during acute hypoglycemia (white arrows). *C*: UCN3 neurons in the MAN (white arrows). *D*: Neuronal cell bodies showing FG (blue), cFOS (green), and UCN3 (red). Triple staining is seen in those neurons identified by white arrows. (A high-quality digital representation of this figure is available in the online issue.)

readings were assessed in this study (31). Food intake was not measured in our study, but we did not find an increase in blood glucose after VMH 5-TG or 2-DG. The reasons for these discrepancies are not clear. Borg et al. (9) used microdialysis to deliver 2-DG locally to the VMH, and it is possible that, under these conditions, the stimulus to glucose-sensing neurons is greater. Interestingly, recurrent glucoprivation impairs hypothalamic but not hindbrain responses to subsequent hypoglycemia (32), suggesting that repeated hypoglycemia restrains hindbrain glucose-sensing via an upstream (hypothalamic and or other brain region) mechanism. On the basis of the present findings and those of Ritter et al. (30), we would speculate that glucose-sensors in the hindbrain may form part of a classical sensory reflex response, whereas glucose-sensors in higher centers are more integrated in their response to a glucoprivation, that is, hypoglycemia might need to be present in a number of glucose-sensing brain and/or peripheral sensors before counterregulation is initiated.

Given the importance of the VMH to the detection of hypoglycemia and our previous studies showing a role for UCN3 in the VMH in modulating the counterregulatory response to hypoglycemia, we then sought to examine whether UCN3 might link these two glucose-sensing regions. Previous neuroanatomical studies have shown that the MAN projects topographically to the VMH (25), findings confirmed in our study using retrograde neural tracers to show reciprocal pathways between these two regions. Additionally, we have been able to demonstrate that most of the UCN3 projections to the VMH arise in the MAN. Moreover, using triple-staining immunohistochemistry, we also found that ~1/3 of these activated during acute hypoglycemia. In this context, our previous finding that pharmacological manipulation of CRH-R2 receptors in the VMH markedly altered counterregulatory responses to acute hypoglycemia is very suggestive of a functional role for this neural network (13). It is perhaps counterintuitive that UCN3 activation in the MAN during hypoglycemia might lead to suppression of glucose-sensing neurons in the VMH. However, it is notable that few of the individual MAN glucose-sensing neurons identified by Ca^{2+} imaging also expressed mRNA for UCN3. On the other hand, many did express mRNA for its receptor, CRH-R2. In addition, gene expression analysis from serial MAN micropunches showed that glucokinase and CRH-R2 gene expression had the same rostrocaudal distribution, but the opposite rostrocaudal distribution as UCN3 mRNA. This implies that UCN3 neurons may represent a discrete neuronal population in the MAN that are not in themselves glucose-sensing and, thus, may also directly regulate glucose-sensing neurons locally, as they do in the VMH. This would lead us to speculate that UCN3 neurons may regulate or coordinate the output, in terms of the counterregulatory responses, from these two discrete glucose-sensing regions.

In summary, in the current study we have identified the MAN as a novel limbic glucose-sensing region that contains characteristic glucokinase-expressing glucose-sensing neurons that respond directly to manipulations of glucose availability. In addition, manipulation of the MAN by lesion or through provision of an additional glucoprivic

stimulus modulates the counterregulatory response to moderate systemic hypoglycemia. Finally, we have shown that both these glucose-sensing regions are linked by UCN3 neurons, which potentially provides a mechanism for fine-tuning and integrating the stress response during a hypoglycemic challenge.

ACKNOWLEDGMENTS

This work was supported by National Institutes of Health Grants (DK-069831, R.J.M.) and (DK-53181, B.E.L.), the Diabetes and Endocrinology Research Center (DERC) at Yale, and the Juvenile Diabetes Research Foundation (R.J.M.). L.Z. is a Juvenile Diabetes Research Foundation Postdoctoral Research Fellow. B.E.L. is supported by the Research Service of the Veterans Administration.

No potential conflicts of interest relevant to this article were reported.

L.Z. conducted the in vivo studies and performed IHC; N.P. performed the fura-2 calcium imaging and sc-QPCR; Z.S. helped with the in vivo studies and IHC; Y.D. performed rodent surgeries and helped with in vivo studies; X.F. helped with in vivo studies; Q.T. contributed to the discussion; B.E.L. supervised fura-2 calcium imaging and sc-QPCR, helped with manuscript preparation, and contributed to the discussion; R.J.M. wrote the manuscript and designed and supervised the in vivo studies and IHC.

The authors are grateful to Ralph Jacob and Aida Groszmann, Yale University, for their support and assistance. The authors thank Dr. Wylie Vale, Salk Institute, CA, for kindly providing the Urocortin 3 antibody used in these studies, and Dr. Brad Lowell, Beth Israel Deaconness Medical Center, Boston, MA, for his helpful comments.

REFERENCES

1. McCrimmon R. Glucose sensing during hypoglycemia: lessons from the lab. Diabetes Care 2009;32:1357–1363
2. Levin BE, Routh VH, Kang L, Sanders NM, Dunn-Meynell AA. Neuronal glucosensing: what do we know after 50 years? Diabetes 2004;53:2521–2528
3. Routh VH. Glucose-sensing neurons: are they physiologically relevant? Physiol & Behav 2002;76:403–413
4. Canabal DD, Song Z, Potian JG, Beuve A, McArdle JJ, Routh VH. Glucose, insulin, and leptin signaling pathways modulate nitric oxide synthesis in glucose-inhibited neurons in the ventromedial hypothalamus. Am J Physiol Regul Integr Comp Physiol. 2007;292:R1418–1428
5. Fioramonti X, Marsollier N, Song Z, Fakira KA, Patel RM, Brown S, Duparc T, Pica-Mendez A, Sanders NM, Knauf C, Valet P, McCrimmon RJ, Beuve A, Magnan C, Routh VH. Ventromedial hypothalamic nitric oxide production is necessary for hypoglycemia detection and counterregulation. Diabetes 2010;59:519–528
6. Kang L, Dunn-Meynell AA, Routh VH, Gaspers LD, Nagata Y, Nishimura T, Eiki J, Zhang BB, Levin BE. Glucokinase is a critical regulator of ventromedial hypothalamic neuronal glucosensing. Diabetes 2006;55:412–420 [Erratum appears in Diabetes 2006;55(3):862]
7. Borg MA, Sherwin RS, Borg WP, Tamborlane WV, Shulman GI. Local ventromedial hypothalamus glucose perfusion blocks counterregulation during systemic hypoglycemia in awake rats. J Clin Invest 1997;99:361–365
8. Borg WP, During MJ, Sherwin RS, Borg MA, Brines ML, Shulman GI. Ventromedial hypothalamic lesions in rats suppress counterregulatory responses to hypoglycemia. J Clin Invest 1994;93:1677–1682
9. Borg WP, Sherwin RS, During MJ, Borg MA, Shulman GI. Local ventromedial hypothalamus glucopenia triggers counterregulatory hormone release. Diabetes 1995;44:180–184
10. Evans SB, Wilkinson CW, Gronbeck P, Bennett JL, Taborsky GJ, Jr, Figlewicz DP. Inactivation of the PVN during hypoglycemia partially simulates hypoglycemia-associated autonomic failure. Am J Physiol Regul Integr Comp Physiol 2003;284:R57–65
11. Evans SB, Wilkinson CW, Gronbeck P, Bennett JL, Zavosh A, Taborsky GJ, Jr, Figlewicz DP. Inactivation of the DMH selectively inhibits the ACTH and corticosterone responses to hypoglycemia. Am J Physiol Regul Integr Comp Physiol 2004;286:R123–128
12. Cheng H, Zhou L, Zhu W, Wang A, Tang C, Chan O, Sherwin RS, McCrimmon RJ. Type 1 corticotropin-releasing factor receptors in the ventromedial hypothalamus promote hypoglycemia-induced hormonal counterregulation. Am J Physiol Endocrinol Metab 2007;293:E705–712
13. McCrimmon RJ, Song Z, Cheng H, McNay EC, Weikart-Yeckel C, Fan X, Routh VH, Sherwin RS. Corticotrophin-releasing factor receptors within the ventromedial hypothalamus regulate hypoglycemia-induced hormonal counterregulation. J Clin Invest 2006;116:1723–1730
14. Li C, Vaughan J, Sawchenko PE, Vale WW. Urocortin III-immunoreactive projections in rat brain: partial overlap with sites of type 2 corticotrophin-releasing factor receptor expression. Journal of Neuroscience 2002;22:991–1001
15. Lynch RM, Tompkins LS, Brooks HL, Dunn-Meynell AA, Levin BE. Localization of glucokinase gene expression in the rat brain. Diabetes 2000;49:693–700
16. Rossetti L, Shulman GI, Zawalich W, DeFronzo RA. Effect of chronic hyperglycemia on in vivo insulin secretion in partially pancreatectomized rats. J Clin Invest 1987;80:1037–1044
17. Powell AM, Sherwin RS, Shulman GI. Impaired hormonal responses to hypoglycemia in spontaneously diabetic and recurrently hypoglycemic rats. Reversibility and stimulus specificity of the deficits. J Clin Invest 1993;92:2667–2674
18. Zhou L, Furuta T, Kaneko T. Chemical organization of projection neurons in the rat accumbens nucleus and olfactory tubercle. Neuroscience 2003;120:783–798
19. Zhou L, Furuta T, Kaneko T. Neurokinin B-producing projection neurons in the lateral stripe of the striatum and cell clusters of the accumbens nucleus in the rat. J Comp Neurol 2004;480:143–161
20. Paxinos G, Watson C. *The Rat Brain in Stereotaxic Coordinates*. San Diego, CA, Academic Press, 1997
21. Palkovits M. Isolated removal of hypothalamic or other brain nuclei of the rat. Brain Res 1973;59:449–450
22. Levin BE, Dunn-Meynell AA, Ricci MR, Cummings DE. Abnormalities of leptin and ghrelin regulation in obesity-prone juvenile rats. Am J Physiol Endocrinol Metab 2003;285:E949–957
23. Kang L, Routh VH, Kuzhikandathil EV, Gaspers LD, Levin BE. Physiological and molecular characteristics of rat hypothalamic ventromedial nucleus glucosensing neurons. Diabetes 2004;53:549–559
24. Liss B. Improved quantitative real-time RT-PCR for expression profiling of individual cells. Nucleic Acid Res 2002;30:e89
25. Canteras NS, Simerly RB, Swanson LW. Organization of projections from the medial nucleus of the amygdala: a PHAL study in the rat. J Comp Neurol 1995;360:213–245
26. King BM. The rise, fall, and resurrection of the ventromedial hypothalamus in the regulation of feeding behavior and body weight. Physiol Behav 2006;87:221–244
27. Dunn JT, Cranston I, Marsden PK, Amiel SA, Reed LJ. Attenuation of amydgala and frontal cortical responses to low blood glucose concentration in asymptomatic hypoglycemia in type 1 diabetes: a new player in hypoglycemia unawareness? Diabetes 2007;56:2766–2773
28. McCrimmon R. The mechanisms that underlie glucose sensing during hypoglycaemia in diabetes. Diabet Med 2008;25:513–522
29. Dunn-Meynell AA, Routh VH, Kang L, Gaspers L, Levin BE. Glucokinase is the likely mediator of glucosensing in both glucose-excited and glucose-inhibited central neurons. Diabetes 2002;51:2056–2065
30. Ritter S, Dinh TT, Zhang Y. Localization of hindbrain glucoreceptive sites controlling food intake and blood glucose. Brain Res 2000;856:37–47
31. Dunn-Meynell AA, Sanders NM, Compton D, Becker TC, Eiki J, Zhang BB, Levin BE. Relationship among brain and blood glucose levels and spontaneous and glucoprivic feeding. J Neurosci 2009;29:7015–7022
32. Sanders NM, Taborsky GJ, Jr, Wilkinson CW, Daumen W, Figlewicz DP. Antecedent hindbrain glucoprivation does not impair the counterregulatory response to hypoglycemia. Diabetes 2007;56:217–223